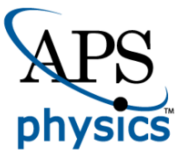

This is the accepted manuscript made available via CHORUS. The article has been published as:

New Precision Limit on the Strange Vector Form Factors of the Proton

Z. Ahmed *et al.* (HAPPEX Collaboration)

Phys. Rev. Lett. **108**, 102001 — Published 5 March 2012

DOI: 10.1103/PhysRevLett.108.102001

New Precision Limit on the Strange Vector Form Factors of the Proton

(The HAPPEX Collaboration)

Z. Ahmed,[1] K. Allada,[2] K. A. Aniol,[3] D. S. Armstrong,[4] J. Arrington,[5] P. Baturin,[6] V. Bellini,[7] J. Benesch,[8] R. Beminiwattha,[9] F. Benmokhtar,[10] M. Canan,[11] A. Camsonne,[8] G. D. Cates,[12] J.-P. Chen,[8] E. Chudakov,[8] E. Cisbani,[13] M. M. Dalton,[12] C. W. de Jager,[8,12] R. De Leo,[14] W. Deconinck,[4] P. Decowski,[15] X. Deng,[12] A. Deur,[8] C. Dutta,[2] G. B. Franklin,[10] M. Friend,[10] S. Frullani,[13] F. Garibaldi,[13] A. Giusa,[7] A. Glamazdin,[16] S. Golge,[11] K. Grimm,[17] O. Hansen,[8] D. W. Higinbotham,[8] R. Holmes,[1] T. Holmstrom,[18] J. Huang,[19] M. Huang,[20] C. E. Hyde,[11,21] C. M. Jen,[1] G. Jin,[12] D. Jones,[12] H. Kang,[22] P. King,[9] S. Kowalski,[19] K. S. Kumar,[23] J. H. Lee,[4,9] J. J. LeRose,[8] N. Liyanage,[12] E. Long,[24] D. McNulty,[23] D. Margaziotis,[3] F. Meddi,[25] D. G. Meekins,[8] L. Mercado,[23] Z.-E. Meziani,[26] R. Michaels,[8] C. Muñoz-Camacho,[21] M. Mihovilovic,[27] N. Muangma,[19] K. E. Myers,[28] S. Nanda,[8] A. Narayan,[29] V. Nelyubin,[12] Nuruzzaman,[29] Y. Oh,[22] K. Pan,[19] D. Parno,[10] K. D. Paschke,[12,*] S. K. Phillips,[30] X. Qian,[20] Y. Qiang,[20] B. Quinn,[10] A. Rakhman,[1] P. E. Reimer,[5] K. Rider,[18] S. Riordan,[12] J. Roche,[9] J. Rubin,[5] G. Russo,[7] K. Saenboonruang,[12] A. Saha,[8,†] B. Sawatzky,[8] R. Silwal,[12] S. Sirca,[27] P. A. Souder,[1] M. Sperduto,[7] R. Subedi,[12] R. Suleiman,[8] V. Sulkosky,[19] C. M. Sutera,[7] W. A. Tobias,[12] G. M. Urciuoli,[25] B. Waidyawansa,[9] D. Wang,[12] J. Wexler,[23] R. Wilson,[31] B. Wojtsekhowski,[8] X. Zhan,[19] X. Yan,[32] H. Yao,[26] L. Ye,[33] B. Zhao,[4] and X. Zheng[12]

[1]*Syracuse University, Syracuse, New York 13244, USA*
[2]*University of Kentucky, Lexington, Kentucky 40506, USA*
[3] *California State University, Los Angeles, Los Angeles, California 90032, USA*
[4]*College of William and Mary, Williamsburg, Virginia 23187, USA*
[5]*Argonne National Laboratory, Argonne, Illinois, 60439, USA*
[6]*Florida International University, Miami, Florida 33199, USA*
[7]*Istituto Nazionale di Fisica Nucleare, Dipt. di Fisica dell'Univ. di Catania, I-95123 Catania, Italy*
[8]*Thomas Jefferson National Accelerator Facility, Newport News, Virginia 23606, USA*
[9]*Ohio University, Athens, Ohio 45701, USA*
[10]*Carnegie Mellon University, Pittsburgh, Pennsylvania 15213, USA*
[11]*Old Dominion University, Norfolk, Virginia 23529, USA*
[12]*University of Virginia, Charlottesville, Virginia 22904, USA*
[13]*INFN, Sezione di Roma, gruppo Sanità and Istituto Superiore di Sanità, I-00161 Rome, Italy*
[14]*Università di Bari, I-70126 Bari, Italy*
[15]*Smith College, Northampton, Massachusetts 01063, USA*
[16]*Kharkov Institute of Physics and Technology, Kharkov 61108, Ukraine*
[17]*Louisiana Technical University, Ruston, Louisiana 71272, USA*
[18]*Longwood University, Farmville, Virginia 23909, USA*
[19]*Massachusetts Institute of Technology, Cambridge, Massachusetts 02139, USA*
[20]*Duke University, Durham, North Carolina 27708, USA*
[21]*Clermont Université, Université Blaise Pascal, CNRS/IN2P3, Laboratoire de Physique Corpusculaire, FR-63000 Clermont-Ferrand, France*
[22]*Seoul National University, Seoul 151-742, South Korea*
[23]*University of Massachusetts Amherst, Amherst, Massachusetts 01003, USA*
[24]*Kent State University, Kent, Ohio 44242, USA*
[25]*INFN, Sezione di Roma and Sapienza - Università di Roma, I-00161 Rome, Italy*
[26]*Temple University, Philadelphia, Pennsylvania 19122, USA*
[27]*Institut Jožef Stefan, 3000 SI-1001 Ljubljana, Slovenia*
[28]*George Washington University, Washington, District of Columbia 20052, USA*
[29]*Mississippi State University, Starkeville, Mississippi 39762, USA*
[30]*University of New Hampshire, Durham, New Hampshire 03824, USA*
[31]*Harvard University, Cambridge, Massachusetts 02138, USA*
[32]*University of Science and Technology of China, Hefei, Anhui 230026, P.R. China*
[33]*China Institute of Atomic Energy, Beijing, 102413, P. R. China*

The parity-violating cross-section asymmetry in the elastic scattering of polarized electrons from unpolarized protons has been measured at a four-momentum transfer squared $Q^2 = 0.624$ GeV^2 and beam energy $E_b = 3.48$ GeV to be $A_{PV} = -23.80 \pm 0.78(\text{stat}) \pm 0.36(\text{syst})$ parts per million. This result is consistent with zero contribution of strange quarks to the combination of electric and magnetic form factors $G_E^s + 0.517\, G_M^s = 0.003 \pm 0.010(\text{stat}) \pm 0.004(\text{syst}) \pm 0.009(\text{ff})$, where the third error is due to the limits of precision on the electromagnetic form factors and radiative corrections. With this measurement, the world data on strange contributions to nucleon form factors are seen to be consistent with zero and not more than a few percent of the proton form factors.

PACS numbers: 13.60.Fz, 11.30.Er, 13.40.Gp, 14.20.Dh

It has long been established that a complete characterization of nucleon substructure must go beyond three valence quarks and include the $q\bar{q}$ sea and gluons. In deep inelastic scattering, for example, sea quarks are known to dominate interactions in certain kinematic regimes. With the discovery by the EMC collaboration [1] that quark spins are not the dominant contribution to nucleon spin, the role of sea quarks, and especially strange quarks, has been scrutinized. More generally, since valence-quark masses account for only about 1% of the nucleon mass, a better understanding of the role of gluons and sea quarks in nucleon substructure is imperative. Cleanly isolating the effects of the quark sea is typically difficult; one notable exception is the extraction of the vector strange matrix elements $\langle \overline{s}\gamma_\mu s\rangle$ in semi-leptonic neutral weak scattering [2].

A quantitative understanding of the role of strange quarks in the nucleon would have broad implications. The range of uncertainty in the strange-quark condensate $\langle \overline{s}s\rangle$ leads to an order of magnitude uncertainty in spin-independent scattering rates of dark matter candidates, while spin-dependent rates are uncertain to a factor of two given the range of uncertainty in the strange-quark contribution to nucleon spin, Δs [3]. The strange-sea asymmetry $s - \overline{s}$ is important for the interpretation of the NuTeV experiment [4, 5]. A better understanding of strangeness in the nucleon will clarify issues for many specific experiments as well as improve our understanding of the role of sea quarks in general.

Following the recognition that parity-violating electron scattering can measure the neutral weak form factors and hence the vector strange-quark matrix elements [6], numerous experiments have been performed. Several such experiments presented evidence supporting non-zero strange form factors, although the significance of the effect was limited [7–9]. In contrast, the HAPPEX collaboration has found results consistent with zero strangeness in each of several measurements at various values of the four-momentum transfer squared Q^2 [10, 11]. The HAPPEX measurements, while only capable of measuring a single value of Q^2 at a time, have put particular emphasis on high statistical accuracy and small systematic uncertainties.

In this paper, we report a new measurement performed in Hall A at Jefferson Laboratory. The kinematics of the measurement were chosen to be particularly sensitive to the apparent effects reported in [7]. The experimental technique was similar to previous HAPPEX measurements [10]. A 100 μA continuous electron beam of longitudinally polarized electrons at 3.481 GeV was incident on a 25 cm long liquid hydrogen target. The twin Hall A High Resolution Spectrometers (HRS) [12] each accepted scattered electrons over a solid angle of 5 msr with an averaged polar angle of $\langle\theta\rangle \sim 13.7^\circ$. Electrons which scattered elastically from protons were focused onto a calorimeter in each spectrometer; electrons from inelastic processes on free protons were not transported to the focal plane. Each calorimeter was composed of alternating layers of lead and lucite, with Čerenkov light from the electromagnetic shower collected by a single photomultiplier tube.

The polarized beam is generated through photoemission from a doped GaAs superlattice crystal. The polarization state of the electron beam was held constant for a time window of about 33 ms, then flipped to the complementary state. The polarities of these pairs of time windows were selected from a pseudorandom sequence. The responses of beam monitors and the electron calorimeters were integrated over each period of stable helicity. Periods of instability in the beam, spectrometer, or data acquisition electronics were cut from the accepted data. A total of 29.9×10^6 pairs passed all cuts and formed the final data sample, including 1.0×10^6 pairs in which only one of the two spectrometers was functional.

The helicity-dependent asymmetry in the integrated calorimeter response A_{raw} was computed for each pair of helicity windows. The physics asymmetry A_{PV} is derived after normalization for beam intensity fluctuations, with corrections for background contributions, kinematics normalization, beam polarization, and changes in beam energy and trajectory. The magnitude and estimated uncertainty due to each of these corrections are described below and summarized in Table I.

The laser optics of the polarized source were carefully configured to minimize changes to the electron beam parameters under polarization reversal [13]. A feedback system was used to minimize the helicity-correlated intensity asymmetry of the beam. Averaged over the course of the experimental run, the helicity-correlated asymmetries in the electron beam were 0.20 parts per million (ppm) in intensity, 0.003 ppm in energy, and 3 nm in position.

Due to the symmetric acceptance of the two spectrometers and the small run-averaged values of helicity-correlated beam asymmetries, the cumulative correction due to beam trajectory and energy asymmetry was only 0.016 ± 0.034 ppm. The calorimeter system response was measured to be linear, with an uncertainty of less than 0.5%, through dedicated tests using pulsed LEDs.

Electrons scattered from the aluminum windows of the cryogenic hydrogen vessel were the largest background. Due to the high Q^2, aluminum elastic scattering did not contribute significantly, leaving quasielastic scattering as the dominant background source. The contributed signal fraction was determined to be $(1.15 \pm 0.35)\%$ using the evacuated target cell to directly measure the aluminum-scattered rate; these rates were checked using

aluminum targets matched to the full target radiation length. The asymmetry of this background was calculated to be -34.5 ppm, with an uncertainty of 30% to account for potential contributions from inelastic states.

Inelastically scattered electrons can also rescatter in the spectrometer and produce a signal in the calorimeter. Dedicated studies of electron rescattering in the spectrometer were combined with parameterizations of the electron-proton inelastic spectra to estimate a fractional contribution of $(0.29 \pm 0.08)\%$ to the total rate. The dominant mechanism was Δ production, for which the theoretical calculated asymmetry of -63 ppm was used with an uncertainty of 20%. An additional systematic uncertainty contribution of 0.14 ppm accounted for the possibility that a small fraction of the signal ($< 10^{-4}$) could have originated from rescattering with ferromagnetic material [10]. The total correction from all sources of background amounted to $(1.0 \pm 0.8)\%$ of A_{PV}.

Both Compton and Møller scattering processes were used to precisely determine the electron beam polarization. The accuracy of the Hall A Møller polarimeter was improved through a careful study of the uniformity of the ferromagnetic foil target, leading to a result of $(89.2 \pm 1.5)\%$. The dominant source of uncertainty in previous analyses of backscattered photons in the Hall A Compton polarimeter [12] lay in the effect of the trigger threshold on the normalization of the analyzing power. This was improved through thresholdless integration of the photon signal, with a result of $(89.41 \pm 0.86)\%$. Averaged, the beam polarization was determined to be $(89.36 \pm 0.75)\%$.

Dedicated low-current data were periodically taken to measure Q^2 using the standard tracking package of the HRS [12]. A water target was used to calibrate the spectrometer angle, with momentum differences from the elastic hydrogen and elastic and inelastic oxygen peaks determining the scattering angle to a precision of 0.4 mrad. Including the spectrometer calibration resolution, the average Q^2 was determined to be $0.624 \pm 0.003\,\mathrm{GeV}^2$, which implies a 0.8% uncertainty on the quoted A_{PV}. An additional correction factor κ, which relates the asymmetry measurement over a finite range of initial-state energy and solid angle to the quoted Q^2, was determined through simulation to be $\kappa = 0.995 \pm 0.002$.

After all corrections to A_{raw}, as summarized in Table I, the parity-violating asymmetry $A_{PV} = -23.80 \pm 0.78\ (\mathrm{stat}) \pm 0.36\ (\mathrm{syst})$ ppm at $Q^2 = 0.624\,\mathrm{GeV}^2$.

Following notation from [9], the theoretical expectation for A_{PV} can be expressed in three terms: $A_{PV} = A_V + A_A + A_S$. A_V and A_A depend on the proton weak charge $(1 - 4\sin^2\theta_W)$ and the nucleon vector and axial-vector electromagnetic form factors, respectively, while strange-quark contributions to the vector form factors are isolated in A_S. At tree level,

$$A_S = A_0 \left[\frac{\epsilon G_E^p G_E^s + \tau G_M^p G_M^s}{\epsilon (G_E^p)^2 + \tau (G_M^p)^2} \right]. \qquad (1)$$

Here $A_0 = G_F Q^2/(4\pi\sqrt{2}\alpha)$, $\tau = Q^2/(4M_p^2)$, $\epsilon = \left[1 + 2(1+\tau)\tan^2(\theta/2)\right]^{-1}$, and $G_{E(M)}^p$ is the proton electric (magnetic) form factor.

$A_{raw} = -21.78 \pm 0.69$ ppm	
Detector Linearity	$0.0\% \pm 0.5\%$
Beam Asymmetries	$-0.9\% \pm 0.2\%$
Backgrounds	$-1.0\% \pm 0.8\%$
Acceptance Factor κ	$-0.5\% \pm 0.2\%$
Beam Polarization	$10.9\% \pm 0.8\%$
Q^2	– $\pm 0.8\%$
Total	$8.5\% \pm 1.5\%$
$A_{PV} = -23.80 \pm 0.78 \pm 0.36$ ppm	

TABLE I: Summary of corrections to the raw asymmetry and the associated systematic uncertainty estimates as a fraction of A_{PV}. The uncertainty on A_{raw} is statistical only, while A_{PV} is listed with statistical and experimental systematic errors.

If strange quarks did not contribute to the vector form factors, the asymmetry at $\langle Q^2 \rangle = 0.624\,\mathrm{GeV}^2$ would be expected to be $A_{NS} = A_V + A_A = -24.062 \pm 0.734$ ppm. This calculation utilizes parameterizations of the electromagnetic form factors which incorporate two-photon-exchange corrections to published form-factor data [14]. The uncertainty in A_{NS} primarily results from uncertainties in these form factors and in radiative corrections in the axial term A_A involving parity-violating multi-quark interactions. While theoretical investigation [15] has suggested that the latter corrections could be as large as 30% of the axial form factor, the net uncertainty in A_{NS} is small for forward-angle studies where the small coefficient $\sqrt{1-\epsilon^2}(1 - 4\sin^2\theta_W)$ suppresses the axial term. The uncertainty in these corrections, as a fraction of the axial form factor, is assumed to be constant with Q^2.

Standard electroweak corrections [16] are also included in the calculation of A_{NS}. Recent improvements to theoretical treatments of γZ box diagrams, evaluated at $Q^2 = 0$, imply a significant additional correction to the proton weak charge [17–20]. This correction is expected to drop with increasing Q^2 [20], suggesting that the correction is suppressed for the measurement reported here. If this expected suppression is ignored, the $Q^2 = 0$ value would imply an increase in the magnitude of A_{NS} by 1.4% at $Q^2 = 0.62\,\mathrm{GeV}^2$, which should be compared to the uncertainty in A_{NS} quoted above as 3.1%. In the absence of a calculation at a Q^2 appropriate to the measurement reported here, this correction is not applied.

Comparing A_{NS} to the measured A_{PV}, the strange-quark contributions are determined to be $G_E^s + 0.517\ G_M^s = 0.003 \pm 0.010 \pm 0.004 \pm 0.009$, where the

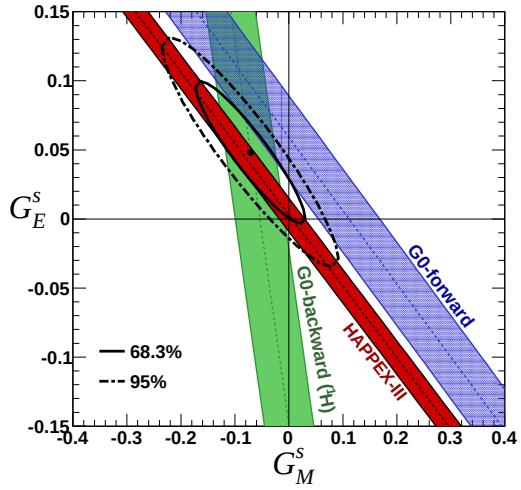

FIG. 1: Constraints on G_E^s and G_M^s at $Q^2 \sim 0.62\,\mathrm{GeV}^2$. The experimental bands are from the results presented in this letter (HAPPEX-III) and the G0 measurements [7, 21].

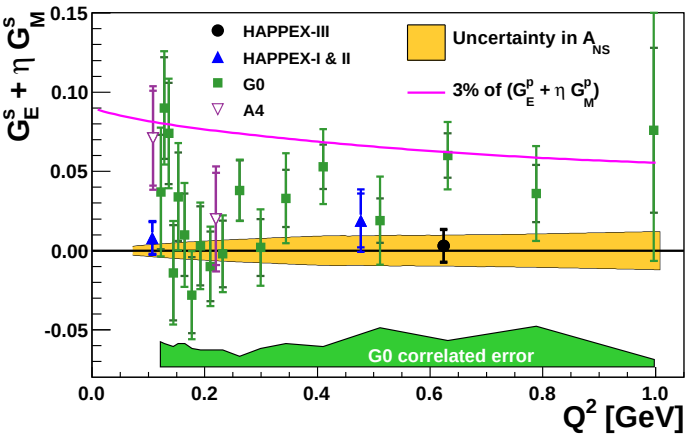

FIG. 2: Results of strange-quark vector form factors for all measurements of forward-angle scattering from the proton. The solid curve represents a 3% contribution to the comparable linear combination of proton form factors.

error bars correspond to statistical, systematic, and the A_{NS} uncertainties, respectively.

The constraints on the 2-D space spanned by G_E^s and G_M^s from all measurements near $Q^2 \sim 0.62\,\mathrm{GeV}^2$ are shown in Fig. 1. The experimental constraints at 1σ are represented by the shaded bands indicating the combined statistical and experimental systematic error bars. The contours, representing the 68% and 95% uncertainty boundaries as indicated, combine all three measurements and also account for the uncertainties in A_{NS}. The independently separated values resulting from this fit are $G_E^s = 0.047 \pm 0.034$ and $G_M^s = -0.070 \pm 0.067$, with a correlation coefficient of -0.93. The combined constraint is consistent with $G_E^s = G_M^s = 0$.

Figure 2 shows all published data on the net strangeness contribution $G_E^s + \eta G_M^s$ in forward-angle scattering measurements from the proton versus Q^2. Here, $\eta = \tau G_M^p/(\epsilon G_E^p)$, and is approximately numerically equal to $Q^2/(\,\mathrm{GeV}^2)$ over the range of the plot. Data from the HAPPEX [10, 11], G0 [7], and A4 [8, 9] collaborations are shown. On each data point, the error bars indicate both the statistical error and the quadrature sum of statistical and uncorrelated systematic error. For the G0 data, some systematic uncertainties are correlated between points with a magnitude indicated by the shaded region at the bottom of the plot. A shaded region around the zero-net-strangeness line represents the uncertainties in A_{NS} at 1σ; this uncertainty is not also included in the individual data points.

While there is no reliable theoretical guidance on the possible Q^2-dependence of the strange form factors, it is reasonable to expect that they would not change rapidly with Q^2, consistent with nucleon form factors in this range which are described to a reasonable precision by smooth dipole or Galster parameterizations [14]. The linear combination of electric and magnetic proton form-factors $G_E^p + \eta G_M^p$, scaled by a factor of 0.03 for convenience, is also plotted for comparison in Fig. 2. The results of this letter rule out large contributions from strange vector form factors with Q^2 behavior similar to that of the nucleon electromagnetic form factors.

This work was supported by the U.S. Department of Energy and National Science Foundation. Jefferson Science Associates, LLC, operates Jefferson Lab for the U.S. DOE under U.S. DOE contract DE-AC05-060R23177.

* Electronic address: paschke@virginia.edu
† Deceased

[1] J. Ashman *et al.* [European Muon Collaboration], Phys. Lett. B **206**, 364 (1988).
[2] D. B. Kaplan and A. Manohar, Nucl. Phys. B **310**, 527 (1988).
[3] J. R. Ellis, K. A. Olive and C. Savage, Phys. Rev. D **77**, 065026 (2008).
[4] H. L. Lai, P. M. Nadolsky, J. Pumplin, D. Stump, W. K. Tung and C. P. Yuan, JHEP **0704**, 089 (2007).
[5] F. Olness *et al.*, Eur. Phys. J. C **40**, 145 (2005).
[6] R. D. McKeown, Phys. Lett. B **219** (1989) 140.
[7] D. S. Armstrong *et al.* [G0 Collaboration], Phys. Rev. Lett. **95**, 092001 (2005).
[8] F. E. Maas *et al.* [A4 Collaboration], Phys. Rev. Lett. **93**, 022002 (2004).
[9] F. E. Maas *et al.* [A4 Collaboration], Phys. Rev. Lett. **94**, 152001 (2005).
[10] K. A. Aniol *et al.* [HAPPEX Collaboration], Phys. Rev. **C69**, 065501 (2004).
[11] A. Acha *et al.* [HAPPEX Collaboration], Phys. Rev. Lett. **98**, 032301 (2007).

[12] J. Alcorn *et al.*, Nucl. Instrum. Meth. **A522**, 294-346 (2004).
[13] K. D. Paschke, Eur. Phys. J. **A32**, 549-553 (2007).
[14] J. Arrington, I. Sick, Phys. Rev. **C76**, 035201 (2007).
[15] S. -L. Zhu, S. J. Puglia, B. R. Holstein, M. J. Ramsey-Musolf, Phys. Rev. **D62**, 033008 (2000).
[16] K. Nakamura *et al.* [Particle Data Group Collaboration], J. Phys. G **G37**, 075021 (2010).
[17] P. G. Blunden, W. Melnitchouk and A. W. Thomas, Phys. Rev. Lett. **107**, 081801 (2011).
[18] A. Sibirtsev, P. G. Blunden, W. Melnitchouk and A. W. Thomas, Phys. Rev. D **82**, 013011 (2010).
[19] B. C. Rislow and C. E. Carlson, Phys. Rev. D **83**, 113007 (2011)
[20] M. Gorchtein, C. J. Horowitz and M. J. Ramsey-Musolf, Phys. Rev. C **84**, 015502 (2011).
[21] D. Androic *et al.* [G0 Collaboration], Phys. Rev. Lett. **104**, 012001 (2010).